ELSEVIER

Fuzzy Sets and Systems 100 (1998) 9–28

FUZZY sets and systems

Application of fuzzy control to a road tunnel ventilation system

Ping-Ho Chen [a], Jiun-Hong Lai [b], Chin-Teng Lin [b,*]

[a] *Section of Control, Department of Electronics, Chung-Shan Institute of Science and Technology, Taoyuan, Taiwan, ROC*
[b] *Department of Control Engineering, National Chiao-Tung University, Hsinchu, Taiwan, ROC*

Received August 1996; revised May 1997

Abstract

This paper deals with the serious problems of ventilation system in a large road tunnel. Higher visibility and lower concentration of carbon monoxide are the key issues concerning the ventilation system. Prior to designing the fuzzy control model, a configuration layout of the ventilation system including sensing, control and traffic prediction as well is conceptually constructed. Based on the layout that offers assignments of sensors and control elements, a fuzzy logic control model is developed. Membership functions of sensor errors and control increments are physically submitted in order to set up the fuzzy logic rules. Timing and spacing filtering in terms of weighting approaches is employed in the fuzzy logic rules. A dynamic equation describing the concentration of air pollution is also given so as to cooperate with the fuzzy logic rules and to play roles in the computer simulation. The result of computer simulation involving five cases indicates that a multi-level scheme is able to solve the engineering problems. © 1998 Elsevier Science B.V. All rights reserved

Keywords: Fuzzy logic control; Tunnels; Ventilation; Simulation; Traffic prediction

1. Introduction

Moving vehicles with speed 80 km/h usually take about 10 min to pass safely along a large road tunnel with 13 km or higher in length stretched and lied on an expressway. In such a long driving duration in those large tunnels, it is necessary to provide a satisfied environment avoid of foreseeable potential hazards. Among those hazards, air pollution is greatly concerned due to its harm to vehicle drivers and passengers. Research of air pollution control in a tunnel ventilation system is thus recognized as a significant topic in case of traffic congestion. The air in the tunnel, usually contaminated by CO, HC and dust, will reduce the visibility and more seriously cause traffic accidents accordingly. The objective of air pollution control is given as follows [1]:

- To increase the visibility so that the visibility index (VI) $\geqslant 40\%$. Actual control scheme regulates VI $\geqslant 50\%$ for safety reason.
- To decrease the concentration of carbon monoxide denoted by CO so that CO < 100 ppm. Actual control scheme regulates CO < 40 ppm.
- To minimize electrical power consumption for cost-effective.

How to get started so as to meet the objectives of pollution control problems as mentioned is a key issue of concern. Two subsystems, Plant Monitor Control System (PMCS) and Traffic Surveillance and Control System (TSCS), are considered in the entire tunnel system [2]. If applied to the tunnel ventilation system, PMCS might deal with the operation and management

* Corresponding author.

PII: S0165-0114(97)00209-1

of the tunnel installation and TSCS handles the traffic monitoring and ventilation control.

An outline of the tunnel ventilation control system using artificial intelligence [3] is referred and remodeled in the following configuration layout for providing a functional environment and thus modeling the dynamics hereafter.

Dynamic description and associated experimental curve or data are employed for computer simulation [4, 5] in which cases to be studied and simulation results to be concluded are schemed corresponding to the actual application results [6]. A thorough ventilation system including plant, dynamics, fuzzy logic control, simulation and evaluation is thus developed as follows.

2. Configuration layout [2]

Prior to designing the fuzzy logic controller, a configuration layout concerning the facility installation, ventilation control and pollutant dynamic should be introduced.

2.1. Configuration of facility installation

The entire tunnel in Fig. 1 is divided into four sections by three vertical shafts, VS1–VS3. Each vertical shaft is equipped with two blowers BO/BI, one of which, the BO blows off the contaminated air from the tunnel into the ambient while the other BI sucks in fresh air from ambient into the tunnel. All the sensors and control elements are installed in each section along the tunnel based on the proposed positioning assignment as follows:

Sensors

(i) Visibility index (VI):
- maximum VI spot
- in front of dust collectors (DC)
- in front of blowers (BL)
- entrance and exit.

(ii) CO counter (CO):
- in front of blowers
- entrance and exit.

(iii) Wind speed (WS):
- each section.

(iv) Traffic counter (TC):
- 1 km aparted.

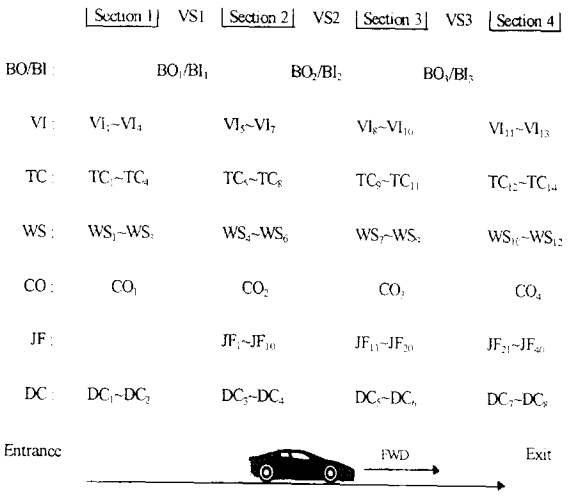

Fig. 1. Configuration of facility installation.

Control elements

(i) Dust collector (DC):
- each section.

(ii) Blower (BO/BI):
- entrance and exit.

(iii) Jet fan (JF):
- section #2, #3, #4.

The number of sensors for VI, TC, WS and CO are 13, 13, 12 and 4, respectively. The number of control elements for BO/BI and JF are 3 and 40, respectively. The length of each section is about 3–3.5 km. Positioning of sensors and control elements will be alluded after introducing pollutant dynamic. Based on this assumed configuration of facility installation, a model of ventilation control system in detail is thus developed as below.

2.2. Configuration of ventilation control system

The configuration of ventilation system as shown in Fig. 2 is composed of six subsystems, i.e. sensing elements (CO counter CO; Visibility index *VI*; Anemometer WS; Traffic counter TC), fuzzy logic control, spacing and timing filter, control elements (Blower BL; Dust collector DC; Jet fan JF), pollutant dynamic and traffic/pollutant predictor. Notation of Fig. 2 is defined as follows:

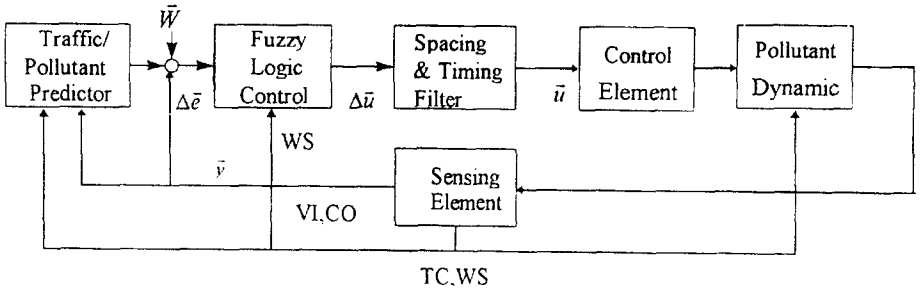

Fig. 2. Configuration of ventilation control.

$\boldsymbol{W}(k)$: Expected values of VI and CO in vector form at each section along the tunnel:

$$\boldsymbol{W}(k) = \langle VI_1(k), \ldots, VI_{13}(k); CO_1(k), \ldots, CO_4(k)\rangle$$
$$= \langle 0.5, \ldots, 0.5; 40, \ldots, 40\rangle \text{ (control objective)}$$

$\boldsymbol{y}(k)$: Measured data of VI and CO in vector form at each section along the tunnel:

$$\boldsymbol{y}(k) = \langle VI_1(k), \ldots, VI_{13}(k); CO_1(k), \ldots, CO_4(k)\rangle$$

$\boldsymbol{e}(k)$: Control error

$$\boldsymbol{e}(k) = \boldsymbol{w}(k) - \boldsymbol{y}(k)$$

$\Delta\boldsymbol{u}(k)$: Increment of control in vector form:

$$\Delta\boldsymbol{u}(k) = \langle \Delta\boldsymbol{N}_{\mathrm{JF}}(k), \Delta\boldsymbol{BL}(k), \Delta\boldsymbol{DC}(k), \Delta\boldsymbol{u}(k-1)\rangle$$
$$\Delta\boldsymbol{N}_{\mathrm{JF}}(k) = \langle \Delta N_{\mathrm{JF}_{1-10}}(k), \Delta N_{\mathrm{JF}_{11-20}}(k),$$
$$\Delta N_{\mathrm{JF}_{21-40}}(k)\rangle;$$
$$\Delta\boldsymbol{BL}(k) = \langle \Delta BL_1(k), \Delta BL_2(k), \Delta BL_3(k)\rangle;$$
$$\Delta\boldsymbol{DC}(k) = \langle \Delta DC_1(k), \ldots, \Delta DC_8(k)\rangle;$$

$\Delta\boldsymbol{N}_{\mathrm{JF}}$ is the number vector increment of operated jet fans at each section.
$\Delta\boldsymbol{BL}$ is the speed vector increment of blowers at each section.

$\boldsymbol{u}(k)$: Control vector $\langle \boldsymbol{N}_{\mathrm{JF}}, \boldsymbol{BL}\rangle$, $\boldsymbol{N}_{\mathrm{JF}}$ is the number vector of operated jet fans at each section and $\boldsymbol{BL}$ is the speed vector of the blowers in each section.

In Fig. 2, the expected values of *VI* and *CO* are to be compared with the sensing value of *VI* and *CO* and/or predicted incremental values of *VI* and *CO*. Errors of *VI* and *CO* are thus generated to activate the fuzzy logic control rules. Output of the fuzzy logic control to be compensated by spacing filters and timing filters will present a more reasonable driving signal for control elements. The relationship between *VI*, *CO* and control elements is described by pollutant dynamic equation as follows.

2.3. Configuration of pollutant distribution

Air pollution caused by moving vehicles is usually consisted of dust, smoke, carbon monoxide and hydrocarbons HC. A generalized dynamic equation for such air pollutants is given as follows [5]:

$$\frac{\partial c}{\partial t} = \frac{\partial}{\partial x}\left(K\frac{\partial c}{\partial x}\right) - U_r\frac{\partial c}{\partial x} + q - q_s, \tag{1}$$

where c is the pollutant concentration, K the diffusion coefficient, U_r the air flow speed (or wind speed) in the tunnel, q the generation rate of pollutant concentration due to vehicle emission, and q_S the removal rate of pollutant concentration due to the operation of jet fan, blower or dust collector.

The term "q_S" in Eq. (1) is a significant excitation that presents the combined effect resulting from the operation of jet fan, blower and dust collector. Therefore jet fans, blowers and dust collectors are introduced as follows.

2.3.1. Jet fan

A jet fan can pump the air from its front to its back. The concentration of *VI* and *CO* is thus reduced in its front while increased in its back so as to comply with the continuity principle of mass transfer. This phenomena is illustrated by Fig. 3. The increased concentration of VI and CO in its back is further moved forward to the exit partly from piston effect of vehicle in the tunnel and partly from the tunnel wind caused

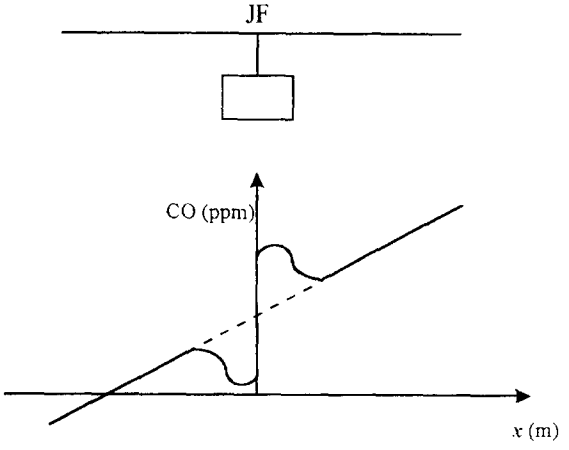

Fig. 3. The concentration of CO in front and in back of jet fan.

by the second jet fan placed at some characteristic length behind. Therefore, the operation of jet fans has effect on the slop of longitudinal distribution curve of the concentration of VI and CO.

2.3.2. Blower

Blowers work as air exchangers to blow the polluted air out to the ambient and blow fresh air into the tunnel. The fresh air may dilute the polluted air right under the vertical shaft and thus reduces the concentration of VI and CO, especially that of CO.

2.3.3. Dust collector

Dust collectors can collect dust in the air and thus increase the visibility under the vertical shaft. Therefore, dust collectors have jump effect on the distribution curve of the concentration of VI rather than that of CO.

3. Positioning of sensors and control elements [3]

The positioning of sensors and control elements depends on the distribution curve of the concentration of VI and CO along the tunnel. Considering the steady state in Eq. (1),

$$\frac{\partial c}{\partial t} = 0 \tag{2}$$

if without operation of control elements,

$$q_s = 0. \tag{3}$$

Eq. (1) can be expressed by

$$k\frac{\partial^2 c}{\partial x^2} - U_r\frac{\partial c}{\partial x} + q = 0. \tag{4}$$

Since the effect of wind speed in the second term is greater than that of diffusion in the first term, i.e.

$$k\frac{\partial^2 c}{\partial x^2} \ll U_r\frac{\partial c}{\partial x}. \tag{5}$$

Therefore, Eq. (4) can be further simplified to the following linear form:

$$\frac{\partial c}{\partial x} = \frac{q}{U_r} \quad \text{or} \quad c(x) = \frac{q}{U_r}x. \tag{6}$$

Eq. (6) shows that the concentration of pollutant is proportional to the distance ahead and the generation rate of pollutant concentration q due to vehicle emission, but inversely proportional to the wind speed U_r. This is an approximate procedure to obtain a linear distribution curve of pollutant concentration. As to the diffusion coefficient k in Eq. (4), it may be found from the transient measurement of distribution curve of pollutant concentration.

Obviously, with known value of q/U_r [4], a linear distribution curve $c(x)$ of pollutant concentration can be found and accordingly, the positioning of sensors (i.e. VI or dust collector) and control elements (i.e. blower or jet fan) can be further decided as follows.

3.1. Positioning of VI sensors

Obviously, the more the number of vehicles in the tunnel, the higher the pollutant concentration and the less the visibility. Therefore, a relationship between the pollutant concentration $c(x)$ and the visibility index $VI(x)$ at steady state can be approximately expressed by

$$VI(x) = VI(0) - kc(x), \tag{7}$$

where $VI(0)$ is the visibility index at the entrance, and k is a coefficient.

The value of VI is expected to be higher than 50% at $x = 1700$ m [4]; therefore,

$$VI(1700) = VI(0) - k\frac{q}{U_r} \times 1700 = 0.5, \tag{8}$$

i.e.

$$k\frac{q}{U_r} = (VI(0) - 0.5)/1700. \tag{9}$$

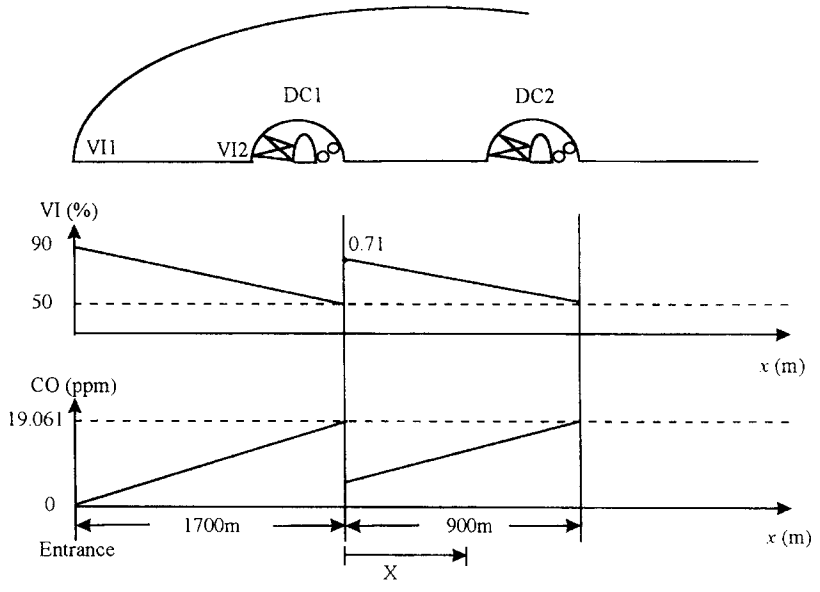

Fig. 4. Longitudinal distribution of CO and VI pollutants at steady state.

The starting value of $VI(0)$ can be obtained from the VI sensor placed at the entrance. Assuming $VI(0)=0.9$, then

$$k\frac{q}{U_r}=0.235\times 10^{-3}(100\%/\mathrm{m}). \tag{10}$$

It means every 1 m apart, the value VI of drops 0.0235%. The nominal wind speed U_r in the tunnel is about 2 m/s. The wind speed is determined by vehicle piston effect, natural wind speed and pumping effect of jet fan. As regard to the generation rate of pollutant concentration q due to vehicle emission, q can be expressed by

$q=$ pollutant concentration per unit volume of
engine emission(ppm/m^3)
$\times$ engine emission rate (m^3/s)
$\times$vehicle occupation (%) (11)

where the emission rate is proportional to vehicle speed V by

$$V(\mathrm{m/min})=QL/\theta, \tag{12}$$

where L is the characteristic length of the vehicle, θ the vehicle occupation and Q the traffic flow.

From the aforementioned scheme, the first VI sensor is placed at the entrance, the second one is placed 1700 m apart together with a dust collector DC_1 as shown in Fig. 4.

3.2. Positioning of dust collector

In order to increase the visibility of driver's vision, dust collectors are applied to absorb smoke and dust in the tunnel. Fig. 4 shows the positioning of DC_1 and DC_2 as proposed in [3]. The efficiency of dust collector is calculated as follows:

For the location at a distance X m behind DC_1,

$$X=x-1700, \tag{13}$$

where x is the distance from the entrance; then

$$VI(x)=VI(X+1700). \tag{14}$$

From Eqs. (8) and (14),

$$VI(X+1700)=VI(1700^+)-0.235\times 10^{-3}X. \tag{15}$$

Let VI = 50% at $X=900$ m; then

$$0.5=VI(1700^+)-0.235\times 10^{-3}\times 900, \tag{16}$$

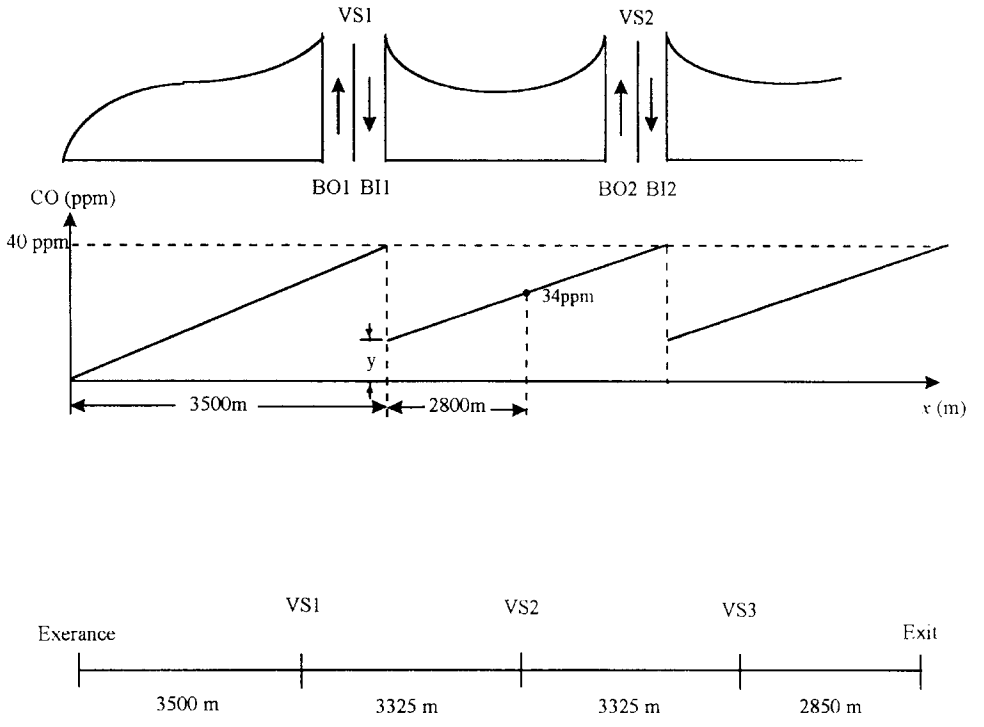

Fig. 5. The position of blowers and vertical shafts along a tunnel.

i.e.

$$VI(1700^{+}) = 0.71 \quad \text{(right behind DC}_1\text{)} \tag{17}$$

but right in front of DC_1, $VI(1700^{-}) = 0.5$.

So the efficiency of VI improvement η_D is

$$\eta_D = \frac{0.71 - 0.5}{0.5} = 42\%. \tag{18}$$

Although the dust collector can improve the visibility, it cannot recover back to 90% of VI as good as at the entrance.

3.3. Positioning of blower

Although the concentration of CO less than 100 ppm is not harmful to vehicle drivers, the performance and control objectives of concentration of CO are set to be less than 50 and 40 ppm, respectively. According to what proposed in Ref. [4], a distribution curve of concentration of CO along a 6300 m (i.e. 3500+2800) tunnel is given as follows:

At the location 3500 m away from the entrance, BO_1/BI_1 in vertical shaft VS_1 reduce the concentration of CO from 40 ppm to some extent say "y" ppm as in Fig. 5. The concentration of CO hereafter increases to 34 ppm at 2800 m behind VS1.

The "y" value is calculated as follows:

$$\frac{40}{3500} = \frac{34 - y}{2800}, \tag{19}$$

i.e.

$$y = 2(\text{ppm}).$$

The efficiency of air exchanging η_B is

$$\eta_B = \frac{40 - 2}{40} \times 100\% = 95\%. \tag{20}$$

In case, there is no operation of jet fan placed between VS_1 and VS_2, the minimum distance D between VS_1 and VS_2 is calculated as follows:

$$\frac{40 - 2}{D} = \frac{40}{3500}, \tag{21}$$

i.e.

$$D = 3325(\text{m}).$$

Fig. 5 shows the positioning of blowers or vertical shafts along a tunnel with 13 km in length.

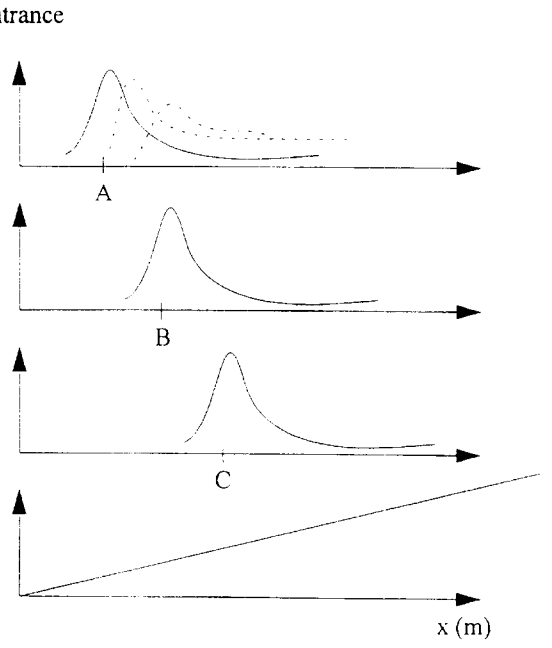

Fig. 6. The pollutant concentration for a single vehicle passing through the tunnel.

3.4. Positioning of jet fan

A single vehicle passing the spot "A" in the tunnel will generate a distribution curve of pollutant concentration just like an impulse response as shown in Fig. 6. As the time elapses, the curve will propagate forward as shown by the dotted lines in Fig. 6. Therefore, for a single vehicle passing through the tunnel, its resulting distribution curve is a combination of each distribution curve, say "A", "B", "C" and so on. Furthermore, for a series of vehicles passing through the tunnel, its overall resulting distribution curve of pollutant concentration is a combination of that of each vehicle. The overall resulting curve of pollutant concentration is approximately a linear curve starting from the entrance. This is the reason why jet fans are uniformly distributed along sections #2, #3, #4 rather than section #1.

4. Fuzzy logic control (FLC)

In order to save power consumption, the control of jet fans and blowers is not continuous but subject to level change over a period of time. This is the reason why the fuzzy logic control (FLC) approach is employed in the controller of this ventilation system. There are three inputs for the FLC, i.e. nominal input, predicted input and sensor feedback input. The nominal input of FLC is the expected values of VI and CO. The predicted input, from the traffic predictor, is the predicted increment of VI and CO. The sensor-feedback input, from the sensors, is measured values of VI and CO. The output of FLC are $\Delta \boldsymbol{N}_{\mathrm{JF}}$, the number vector increment of jet fans and $\Delta \boldsymbol{BL}$, the speed vector increment of blowers. The difference of VI (or CO) as denoted by ΔVI (or ΔCO) is obtained by

$$\Delta VI = \text{measured } VI - (\text{expected } VI + \text{predicted incremental } VI). \tag{22}$$

$\Delta VI, \Delta CO$ accompanied with ΔWS will determine $\Delta \boldsymbol{N}_{\mathrm{JF}}$, the number vector increment of jet fans and $\Delta \boldsymbol{BL}$, the speed vector increment of blowers by means of inference of FLC algorithm. The objective of FLC is to keep the level of VI and CO as required in Fig. 7.

4.1. Membership functions of sensors $\Delta VI, \Delta CO$ and ΔWS

4.1.1. Membership function of ΔVI

The nominal value of VI is set at 50%, the partition boundary is set at ±20% with respect to the nominal value 50%. Therefore, the partition upper bound is 70% and lower bound is 30%. The notation of fuzzy term sets is defined as follows:

PB = Positive Big ($\geqslant 60\%$)

PM = Positive Medium (50–70%)

Z = Zero (40–60%)

NM = Negative Medium (30–50%)

NB = Negative Big ($\leqslant 40\%$)

The membership function of sensors ΔVI is defined in Fig. 8.

4.1.2. Membership functions of ΔCO

The partition boundary of CO is set at ±10 ppm with respect to the nominal value 40 ppm, i.e. the control objective. The upper bound 50 ppm is a satisfying

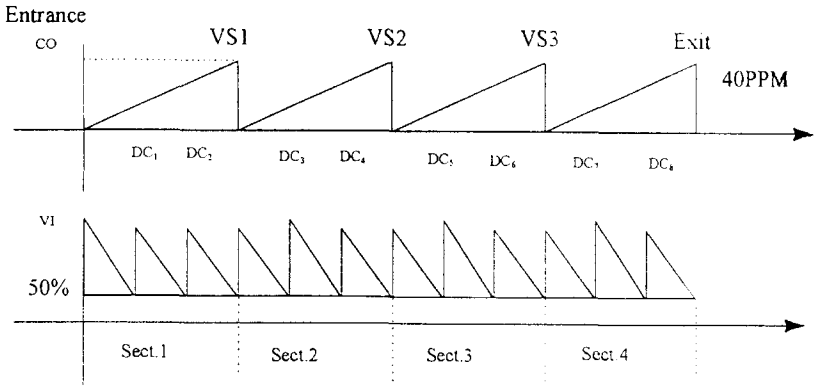

Fig. 7. The objective of FLC of CO and VI at steady state.

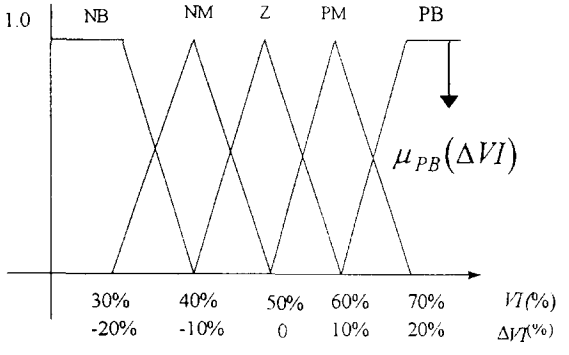

Fig. 8. Membership function of ΔVI.

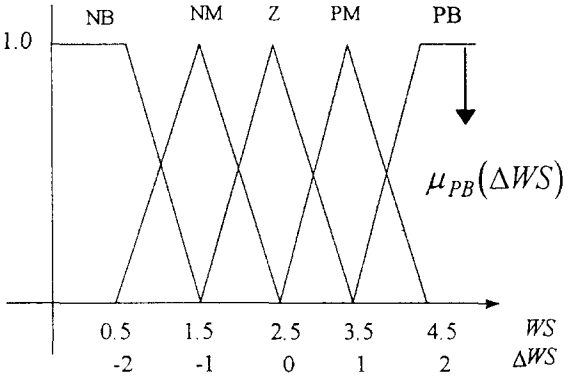

Fig. 10. Membership function of ΔWS.

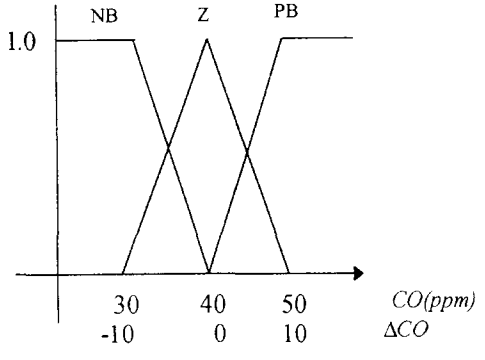

Fig. 9. Membership function of ΔCO.

level of *CO* concentration. Higher than 50 ppm is regarded as a serious level of *CO* concentration. Fig. 9 shows the membership function of ΔCO.

4.1.3. Membership functions of ΔWS

The wind speed in the tunnel is usually 2–3 m/s. The nominal value of *WS* is set at 2.5 m/s with ±2 m/s for upper bound and lower bound. The wind direction is reversed if $\Delta WS < -2.5$ m/s. Fig. 10 shows the membership function of ΔWS.

4.1.4. Membership functions of ΔBO

The air flow rate in the tunnel just in front of vertical shaft VS_1 is assumed 95.8 m^3/s. The air flow rate blew out by BO_1 is assumed 92 m^3/s [4]. Therefore, the air exchanging ratio η_B is

$$\eta_B = \frac{92}{95.8} = 96\%. \tag{23}$$

In other words, there is still 4% residual air remaining in the tunnel. Assuming the characteristic radius R_c of

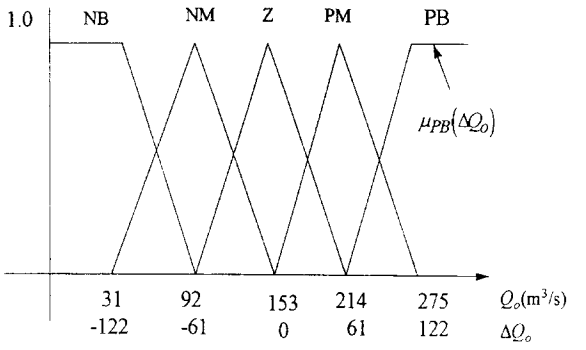

Fig. 11. Membership function of ΔQ_o.

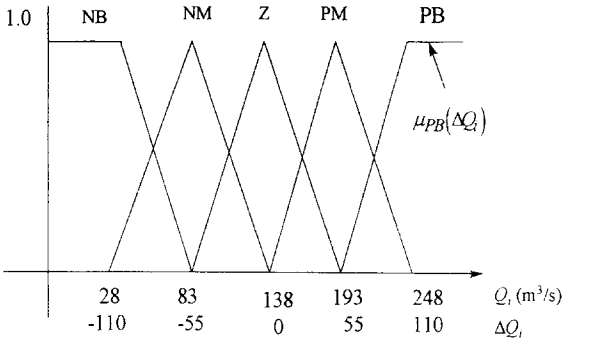

Fig. 12. Membership function of ΔQ_i.

the tunnel is 4.5 m, then its cross section A_T is

$$A_T = \pi R_c^2 = 63.6\,\mathrm{m}^2. \tag{24}$$

For the nominal wind speed V to be 2.5 m/s, the tunnel air flow rate Q_T is

$$Q_T = A_T V = 159\,\mathrm{m}^3/\mathrm{s}. \tag{25}$$

Assuming a vertical shaft with radius r of 3 m, its cross section A_{VS} is

$$A_{VS} = \pi r^2 = 28.3\,\mathrm{m}^2. \tag{26}$$

The air flow rate Q_{VS} in the vertical shaft is

$$Q_{VS} = Q_T \eta_B = 153\,\mathrm{m}^3/\mathrm{s}. \tag{27}$$

The air flow speed in the vertical shaft is

$$V_{VS} = Q_{VS}/A_{VS} = 153/28.3 = 5.5\,\mathrm{m/s}. \tag{28}$$

The wind speed is 2.5 m/s normally with upper bound 4.5 m/s. The percentage of wind speed change η_W is

$$\eta_W = \frac{4.5 - 2.5}{2.5} \times 100\% = 80\%. \tag{29}$$

Therefore, the upper bound of flow rate in the tunnel Q_u is

$$Q_u = Q_T \times 1.8 = 275(\mathrm{m}^3/\mathrm{s}). \tag{30}$$

The membership function of ΔBO is thus given in Fig. 11. Since the air pressure in the tunnel is higher than that of the ambient air, flow rate is Q_i of the blower BI is less than that of BO by almost 10%. The membership of ΔQ_i is thus given in Fig. 12.

4.1.5. *Membership functions of* ΔN_{JF}

There are totally 40 jet fans positioned along the tunnel with 10's for section #2, 10's for section #3, and 20's for section #4. The nominal number of operated jet fans is 4's for section #2, 4's for section #3, and 8's for section #4. The membership function of ΔN_{JF} is thus given in Fig. 13.

4.2. *Inference of FLC controller*

Basically, the control model of a tunnel ventilation system is a MIMO system since the operation of jet fans has effect on the blower control. In the following simulation, a sequence of steps in each sampled time interval is recommended as below:

- To select ΔN_{JF} by inference of FLC.
- To calculate the air flow (or wind) speed.
- To update the coefficient of pollutant dynamic equation.
- To calculate the longitudinal distribution of pollutant concentration.
- To select $\Delta BO/BI$.

In this way, the sophisticated MIMO system may be reduced to a two-MISO system that has same inputs $\Delta VI, \Delta CO$ and ΔWS but different outputs $\Delta BO/BI$ and ΔN_{JF}, respectively, as shown in Table 1.

Table 1 shows the inference of FLC controller for both blower speed control $\Delta BO/BI$ (i.e. air flow speed) and number control of jet fans ΔN_{JF}. Table 1 shows 37 rules rather than 75 rules since in some cases the level of CO is not taken care. Two rules R_1 and R_2 are selected from Table 1 to show the inference procedure of FLC as follows:

R_1: IF ΔVI is *NB* and ΔWS is *NB* and ΔCO is *PB* THEN ΔN_{JF} is *PB*.

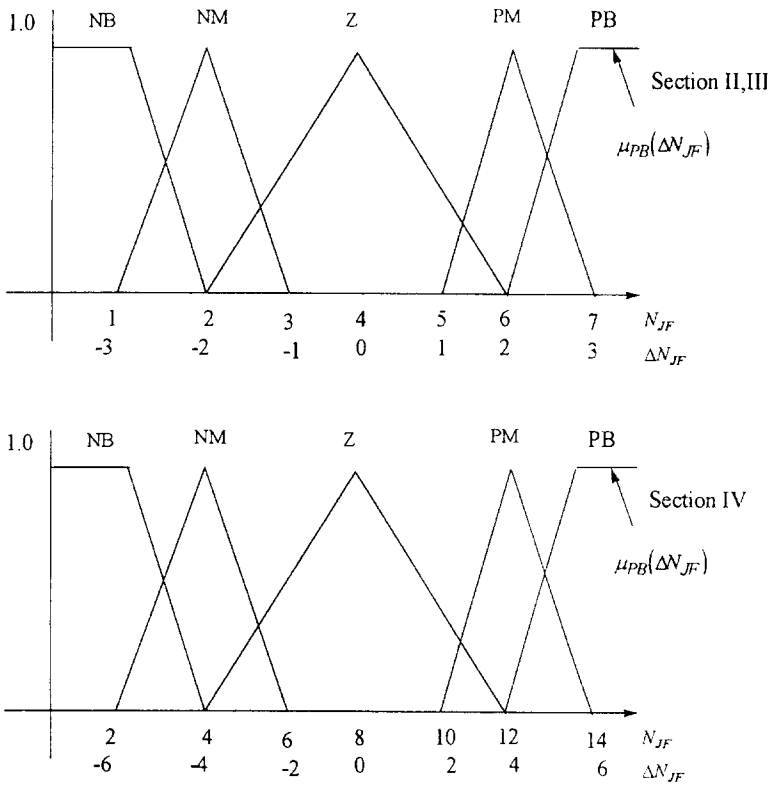

Fig. 13. Membership function of ΔN_{JF}.

Table 1
Inference of FLC controller

ΔWS / ΔVI	*NB*	*NM*	*Z*	*PM*	*PB*
NB	PB, PM, PM	PM	PM	PM	PM, PM, Z
NM	PM	PM	PM	PM, Z, Z	Z
Z	Z	Z	Z	Z	Z
PM	PB, PM, PM	Z, Z, NM	NM	NM	NM
PB	Z, NM, NM	NM	NM	NM	NM, NM, NB

Note: ΔCO is PB, ΔCO is Z, ΔCO is NB.

R_2: IF ΔVI is *NB* and ΔWS is *NB* and ΔCO is *Z* THEN ΔN_{JF} is *PM*.

Based on the following definition:

Input errors e_i $(i = 1, 2, 3)$:

$$e_1 = \Delta VI = VI - VI_{ref}, \quad VI_{ref} = 50\%, \tag{31}$$

$$e_2 = \Delta WS = WS - WS_{ref}, \quad WS_{ref} = 2.5\,\text{m/s}, \tag{32}$$

$$e_3 = \Delta CO = CO - CO_{ref}, \quad CO_{ref} = 40\,\text{ppm}, \tag{33}$$

e_i are error of sensing values.

Linguistic term set of each error:

$$Te_1 = \{x_1 \mid x_1 \in \{NB, NM, Z, PM, PB\}\} \tag{34}$$

$$Te_2 = \{x_2 \mid x_2 \in \{NB, NM, Z, PM, PB\}\} \tag{35}$$

$$Te_3 = \{x_3 \mid x_3 \in \{NB, Z, PM\}\} \tag{36}$$

are linguistic term set of each error.

Membership of each error:

$$\mu_{X_i}(e_i)|_{i=1,2,3}, \tag{37}$$

$$\mu_{T_{e_i}}(e_i) = \bigvee_{X_i} \mu_{X_i}(e_i). \tag{38}$$

Fuzzy singletons:

$$A(e_i) = \begin{cases} 1, & e_i = e_0 \\ 0, & e_i \neq e_0 \end{cases} \quad (i = 1, 2, 3), \tag{39}$$

where e_0 is the measured crispy value.

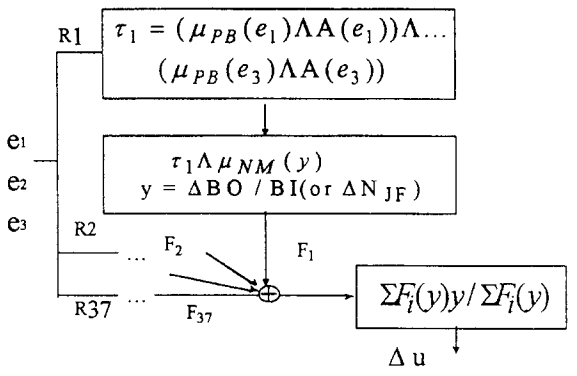

Fig. 14. Defuzzification scheme.

An intersection $M(e_i)$ of the singleton and membership functions is found by

$$M_{T_{e_i}}(e_i) \triangleq \mu_{T_{e_i}}(e_i) \wedge A(e_i)|_{i=1,2,3}. \tag{40}$$

For rule R_1 as shown in Fig. 14, by using max–min algorithm, the degree of fire (DOF) τ_1 is obtained by

$$\tau_1 = \bigwedge_{i}^{3} M_{T_{e_i}}(e_i) \tag{41}$$

4.3. Defuzzification

Using the DOF τ_1 to intersect the membership function of control element $\mu_{T_y}(y)$, a profile of control function $F_1(y)$ is obtained by

$$F_1(y) = \tau_1 \wedge \mu_{T_y}(y). \tag{42}$$

Combining rules R_1 and R_2, a resultant function of control $F_1(y)$ can be found by

$$F(y) = \bigvee_{j=1}^{2} F_j(y) = \bigvee_{j=1}^{2} [\tau_j \wedge \mu_{T_y}(y)]. \tag{43}$$

The above inference is defined in terms of Mamdani's minimum operation rule. Extending to 37 rules of FLC, the resultant function of control is obtained similarly as

$$F(y) = \bigvee_{j=1}^{37} [\tau_j \wedge \mu_{T_y}(y)]. \tag{44}$$

Eq. (44) shows a resultant profile of control function $F(y)$ after finishing the inference of FLC.

The control increment Δu is then acquired in terms of COA (center of area) approach as follows:

$$\Delta u = \frac{\sum F(y)y}{\sum F(y)}. \tag{45}$$

5. Spacing and timing filter for number control of working jet fans (or air-flow control of blowers)

Any one of the measures of ΔVI, ΔWS, ΔCO varies with the location along the tunnel and the time. It is appropriate to express them by $\Delta VI(x,t)$, $\Delta WS(x,t)$, $\Delta CO(x,t)$, respectively. In wide sense, each control element ΔN_{JF} or $\Delta BO/BI$ is not determined exclusively by its local corresponding sensing ΔVI, ΔWS, ΔCO but also counted on the ones in front and the time elapsed as well. Therefore, a spacing/timing filter is thus added on to improved its performance.

5.1. Spacing filter

5.1.1. Sectional average of ΔVI (or ΔWS, ΔCO vice versa)

The sectional average of ΔVI is given as follows:

$$\Delta VI_{\mathrm{AV},i} = \frac{\sum_{j=1}^{k} \Delta VI_{i,j}}{k} \tag{46}$$

where $\Delta VI_{\mathrm{AV},i}$ is the averaged VI value of section # i, ΔVI_{ij} the value of jth VI in section # i and k the number of VI sensors in section # i.

5.1.2. Weighting assignment

After assigning the weighting factors as in Table 2, a spacing filter is constructed as given by

$$\Delta VI_{\mathrm{s},i} = \sum_{j=1}^{i} W_{i,j} \Delta VI_{\mathrm{AV},j} \tag{47}$$

where $\Delta VI_{\mathrm{s},i}$ is ΔVI of section # i after the treatment of space weighting.

5.2. Timing filter

Combining $\Delta VI(x,k)$ and $\Delta VI(x,k-1)$ with time weighting, a timing filter is developed as follows:

$$\Delta VI_{\mathrm{t}}(x,k) = W_{-1}\Delta VI(x,k-1) + W_0 \Delta VI(x,k). \tag{48}$$

Table 2
Weighting table

	Section 2	Section 3	Section 4
$\Delta VI_{AV,1}$	W_{21}	W_{31}	W_{41}
$\Delta VI_{AV,2}$	W_{22}	W_{32}	W_{42}
$\Delta VI_{AV,3}$		W_{33}	W_{43}
$\Delta VI_{AV,4}$			W_{44}

5.3. Resultant filter

The resultant filter is composed of spacing and timing filter as follows:

$$\Delta VI_{R,i} = W_s \Delta VI_{s,i} + W_t \Delta VI_{t,i}, \tag{49}$$

where $\Delta VI_{R,i}$ is the resultant VI of section # i after spacing and timing filter, W_s the weighting factor for sectional spacing filter, W_t the weighting factor for sectional timing filter, $\Delta VI_{s,i}$: ΔVI of section # i after space filtering and $\Delta VI_{t,i}$: ΔVI of section # i after time filtering.

6. Traffic/pollutant predictor

The traffic in the tunnel is usually monitored by vehicle occupation θ, traffic flow Q and associated change rate $\Delta\theta$ and ΔQ in each measured interval. Therefore, a traffic monitoring vector $\boldsymbol{M}$ is introduced by defining

$$\boldsymbol{M} = \langle \theta, \Delta\theta, Q, \Delta Q \rangle, \tag{50}$$

where θ is the vehicle occupation (%) and Q the traffic flow (number of vehicle/min).

Neglecting the diffusion term and time derivative term in Eq. (1) at steady state, Eq. (1) is simplified and expressed as follows:

$$\frac{\partial c}{\partial x} = \frac{q - q_s}{U_r} \tag{51}$$

It is obvious from Eqs. (6) and (51) that the higher traffic flow Q, the more the pollutant generation rate q and the higher the value of $\partial c/\partial x$, spacing rate of pollutant concentration. Jet fans and blowers are thus applied here to remove the pollutant towards the exit. This is an approach to show how the traffic/pollutant predictor works to predict the pollutant concentration in advance based on traffic measures.

7. Computer simulation of FLC ventilation system

7.1. Simplified assumption

As introduced in Section 2.1, there are four sensing elements, i.e. VI (visibility index), CO (CO counter). WS (wind speed), TC (traffic counter) and three control elements, i.e. DC (dust collector), BO/BI (blower) and JF (jet fan). Indeed, the computer simulation will be too huge to be simulated if sensing elements and control elements are all included to cover the longitudinal space of the tunnel and time duration of our concern. Therfore, it is necessary to simplify the approaches of control based on actual physical meaning as follows:

- Operate three blowers (BO/BI) at nominal speed simultaneously if the number control of working jet fans can manage the pollution problems. Otherwise, increase BO/BI to higher speeds, say PM or PB.
- Control the number of working duct collectors (DC) to be synchronized with that of working jet fans due to the linear relationship between VI (effected by DC) and CO (effected by JF).
- Focus on the number control of working jet fans. Define the multi-level control by changing membership function partition, FLC rules or speed of BO/BI to go with working jet fans in terms of the survey of simulation cases.

A simulation scheme is thus simplified by assigning 17 rules for FLC in Table 3 with $\Delta\theta$ (traffic occupation) and ΔCO as input and ΔN_{JF} as output. The following simulation is composed of 10 steps as follows:

Step 1: Generate the traffic flow pattern (associated with TC) by random signal generator at rush hour, say AM 6:00–8:00 and PM 16:00–19:00 as shown in Figs. 16(a) and 17(a).
Step 2: Set initial number N_{JF} of working jet fans.
Step 3: Find wind speed by N_{JF} (piston effect is neglected).
Step 4: Find occupation θ in terms of traffic counter TC.
Step 5: Find the generation rate of pollutant concentration q based on Eq. (10).
Step 6: Find CO by Eq. (6) and ΔCO as well.
Step 7: Find VI by Eq. (13) and ΔVI as well.
Step 8: Estimate occupation θ by Eq. (12) and $\Delta\theta$ as well.

Table 3
General-task FLC rules

IF				THEN
H	Weight	ΔCO	$\Delta\theta$	ΔN_{JF}
1	1	NB	*	NB
2	1	NM	NB	Z
3	1	NM	NM	NM
4	1	NM	Z	NM
5	1	NM	PM	NM
6	1	NM	PB	NB
7	1	Z	NB	PB
8	1	Z	NM	PM
9	1	Z	Z	Z
10	1	Z	PM	Z
11	1	Z	PB	Z
12	1	PM	NB	PB
13	1	PM	NM	PB
14	1	PM	Z	PM
15	1	PM	PM	PM
16	1	PM	PB	PM
17	1	PB	*	PB

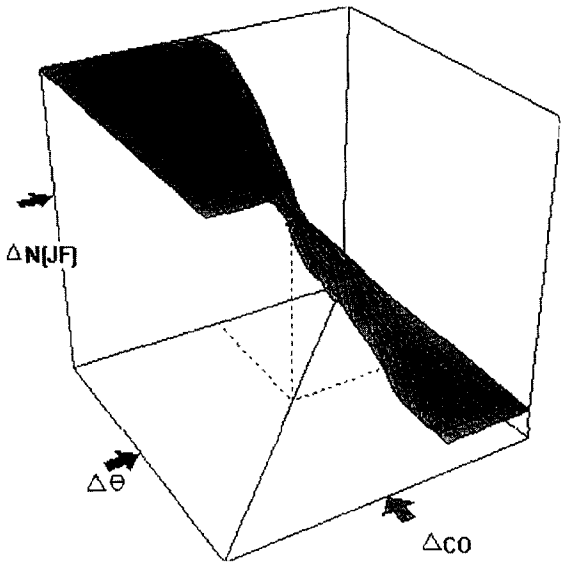

Fig. 15. 3D surface of FLC.

Step 9: Find ΔN_{JF} by ΔCO (from step 6) and $\Delta\theta$ (from step 8).

Step 10: Return to step 3.

The above general-task FLC rules in Table 3 generates a 3D hyperplane surface of FLC as in Fig. 15.

7.2. Cases to be studied

There are five cases to be concerned in the computer simulation:

Case 1: Select hours of traffic jam at AM 6:00 & PM 18:00 and apply the FLC rules table in Table 3, then see if the objective of $CO \leqslant 50$ ppm and $VI \geqslant 40\%$ reaches or not.

Case 2: Change partitions of membership functions for both ΔCO and ΔVI (gain control in other words) and see if the result improves or not.

Case 3: Select one of the most serious problem with higher reverse wind speed at rush hour AM 6:00 and PM 18:00, then check the FLC rules in Table 3 works out or not.

Case 4: Select another serious problem with higher occupation and lower traffic speed (i.e. traffic congestion), then check the FLC rules in Table 3 works out or not.

Case 5: If both Cases 3 and 4 are unable to meet the control objectives for VI and CO, then modify the FLC rules in Table 3.

7.3. Simulation results

Fig. 16 shows a paradigm of generalized simulation results with traffic occupation pattern θ assigned in Fig. 16(a), total number of working jet fans N_{JF} in Fig. 16(b), CO(ppm) concentration in Fig. 16(c) and VI(%) visibility in Fig. 16(d). All the figures are plotted with respect to 24 h time frame.

In order to show the distribution of CO concentration in each section along the tunnel at various time, a 3-D plot of CO vs. time and tunnel sections is given in Fig. 17. Fig. 17 points out that CO concentration sticks up from the allowable objective level of CO concentration at section 1, PM 18:00. This is a generalized case study, called case 1. Obviously, the case 1 result is not so satisfied as expected.

Changing the membership function of ΔCO and $\Delta\theta$ from 500 partitions to 400 partitions, an improvement over case 1 is obtained as shown in Figs. 18 and 19. This is the case 2. CO concentration is satisfied along the tunnel at any time.

In case of serious reverse wind speed, approaches of case 2 no more works out. Figs. 20 and 21 show serious CO pollution. This is the so-called case 3.

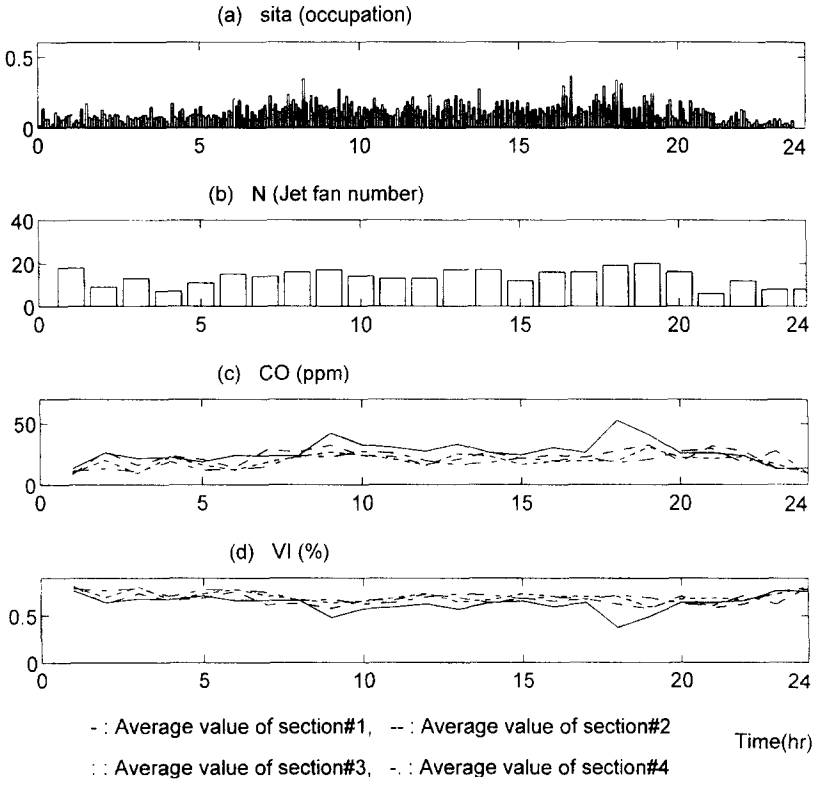

Fig. 16. Simulation results (Case 1).

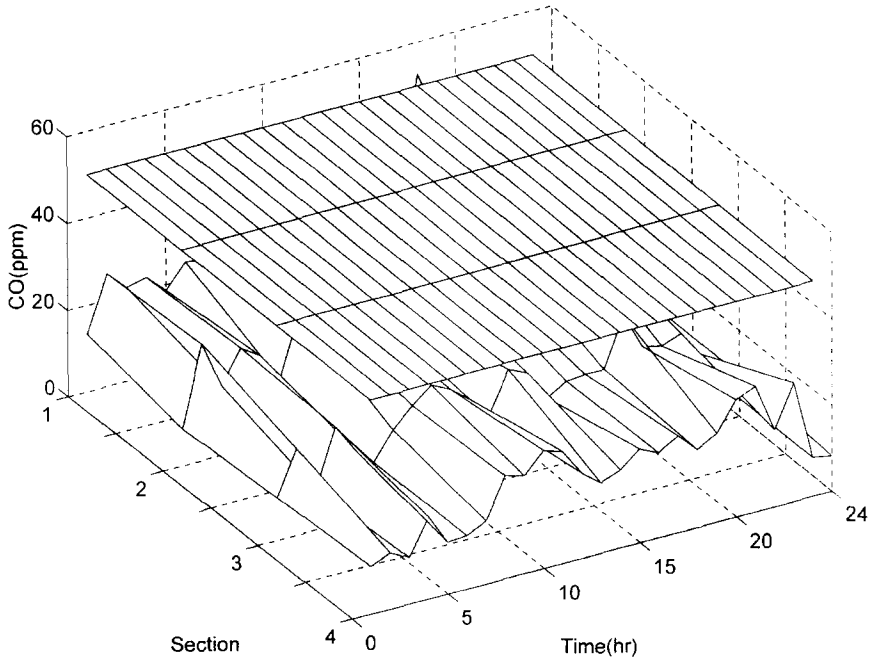

Fig. 17. CO vs. time and tunnel sections (Case 1).

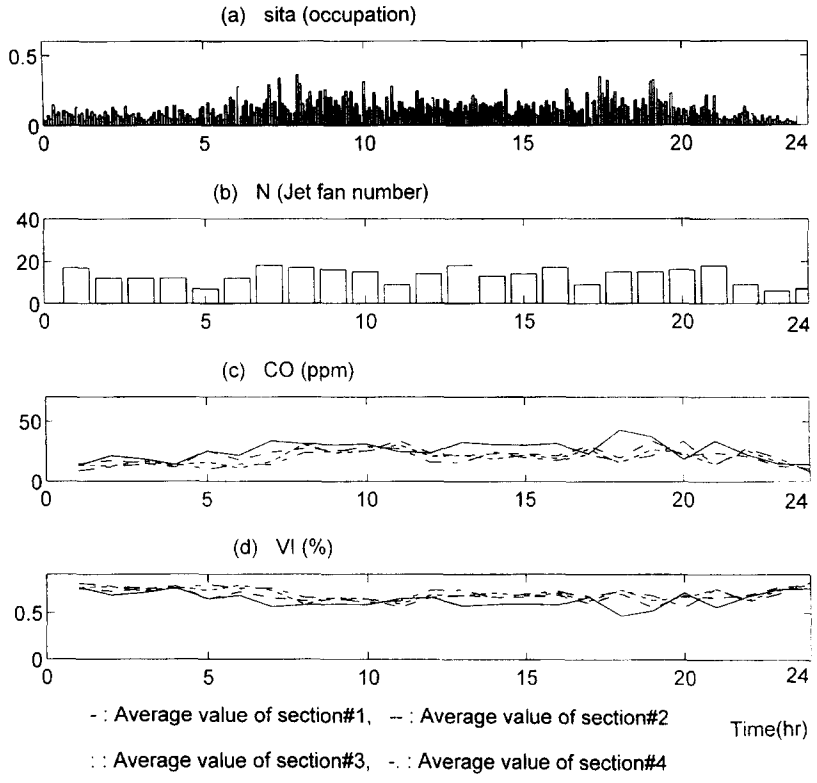

Fig. 18. Simulation results (Case 2).

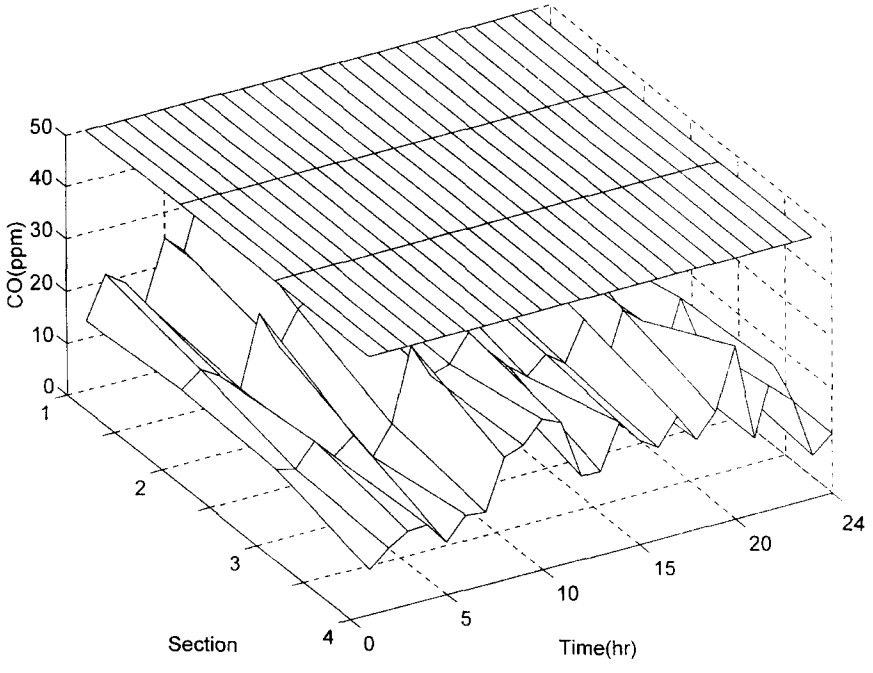

Fig. 19. CO vs. time and tunnel sections (Case 2).

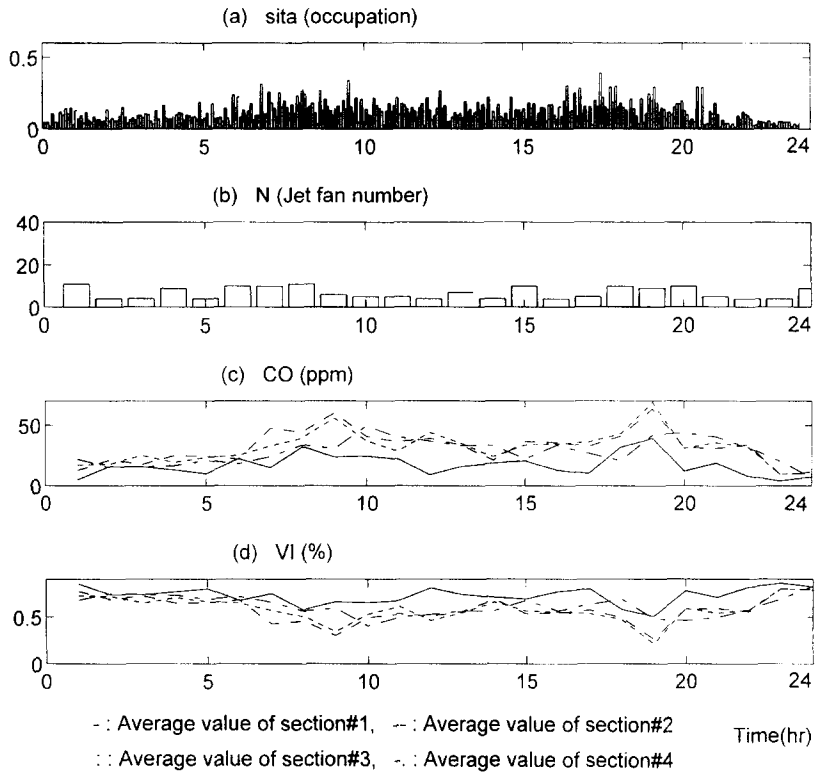

Fig. 20. Simulation results (Case 3).

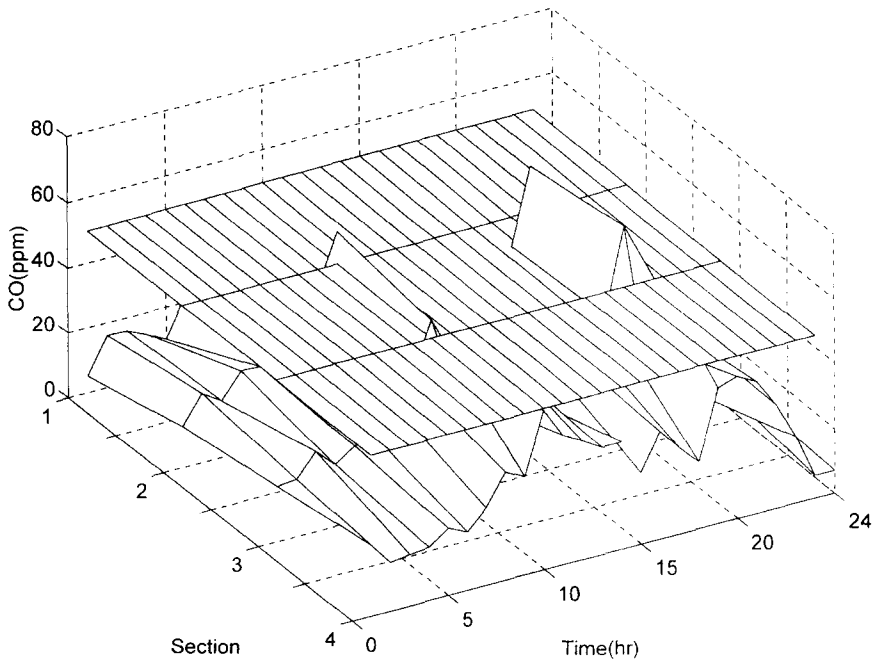

Fig. 21. CO vs. time and tunnel sections (Case 3).

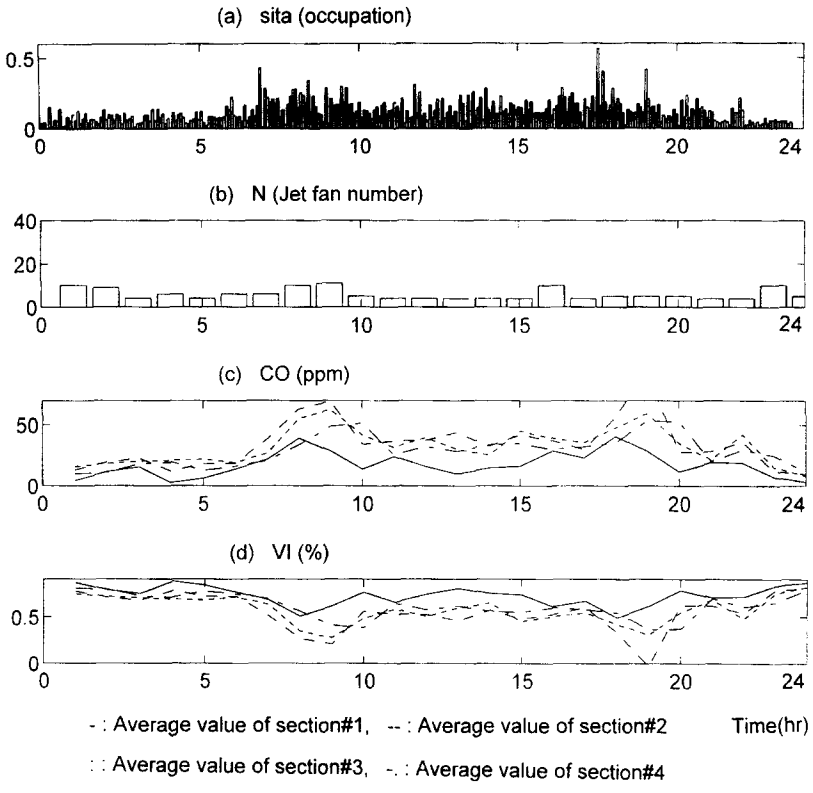

Fig. 22. Simulation results (Case 4).

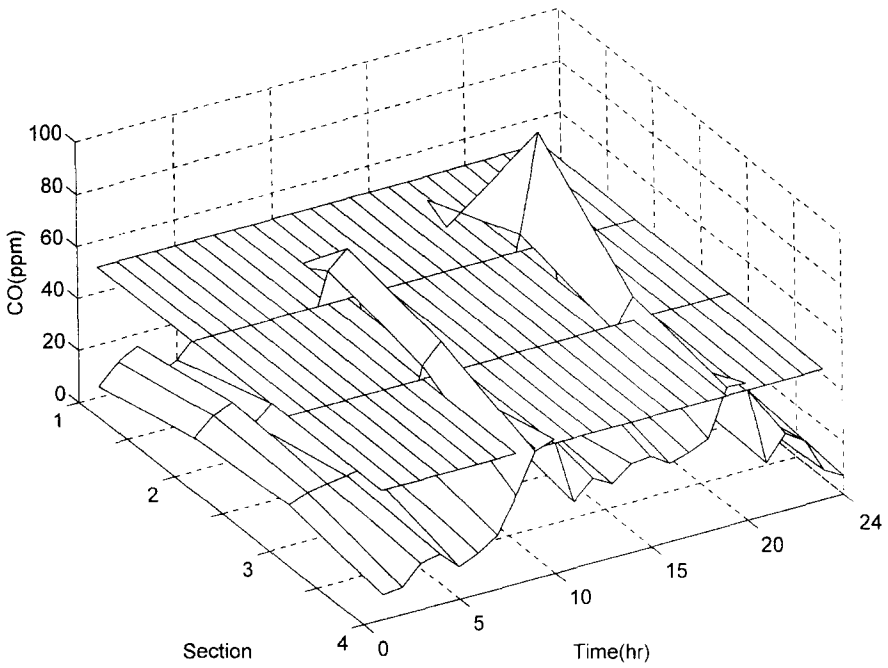

Fig. 23. CO vs. time and tunnel sections (Case 4).

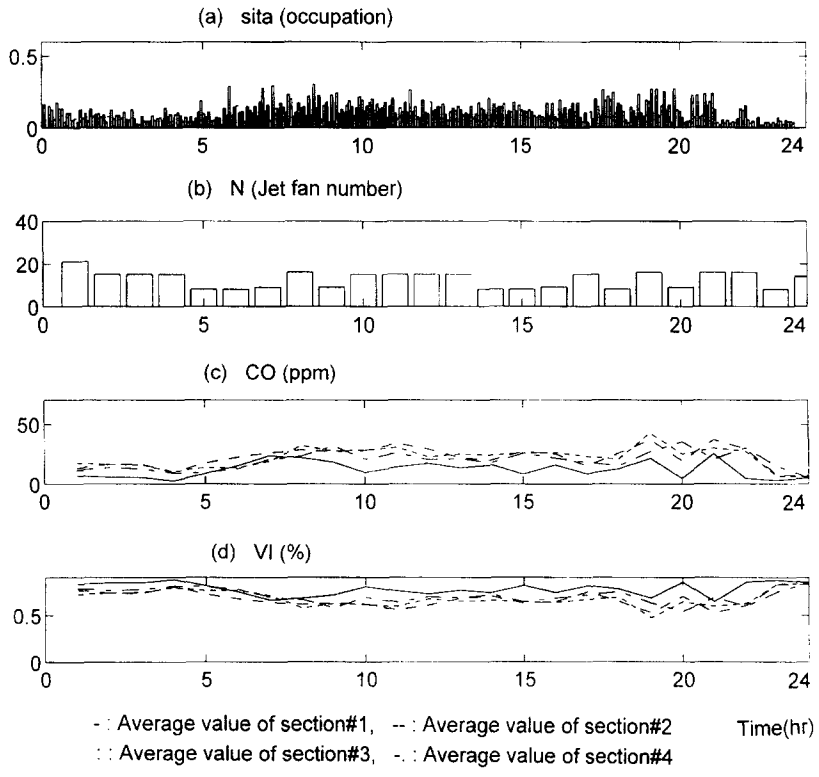

Fig. 24. Simulation results (Case 5).

Table 4
Heavy-task FLC rules

IF				THEN	
H	Weight	ΔCO	$\Delta\theta$	ΔN_{JF}	
1	1	NB	*	NB	
2	1	NM	NB	Z	
3	1	NM	NM	Z	*
4	1	NM	Z	NM	
5	1	NM	PM	NM	
6	1	NM	PB	NB	
7	1	Z	NB	PB	
8	1	Z	NM	PM	
9	1	Z	Z	PM	*
10	1	Z	PM	Z	
11	1	Z	PB	Z	
12	1	PM	NB	PB	
13	1	PM	NM	PB	
14	1	PM	Z	PB	*
15	1	PM	PM	PM	
16	1	PM	PB	PM	
17	1	PB	*	PB	

Furthermore, traffic congestion with higher occupation and lower traffic speed is considered to be case 4. Figs. 22 and 23 show tremendous contamination from CO concentration.

The case combining cases 3 and 4 presents the most serious situation for ventilation control. It is necessary to modify the FLC rules in Table 3 accompanied with changing membership function partition as case 2. The new FLC rules is given in Table 4 for this kind of heavy task.

Observing the difference between Tables 3 and 4, there are 3 rules to be changed as star-marked. This is the so-called case 5. Figs. 24 and 25 associated with case 5 shows that Table 4 is qualified for this kind of heavy-task situation with reverse wind and traffic congestion.

7.4. *Evaluation of performance*

The computer simulation results given in 7.3 reveal that cases 2 and 5 are applicable to general-task and

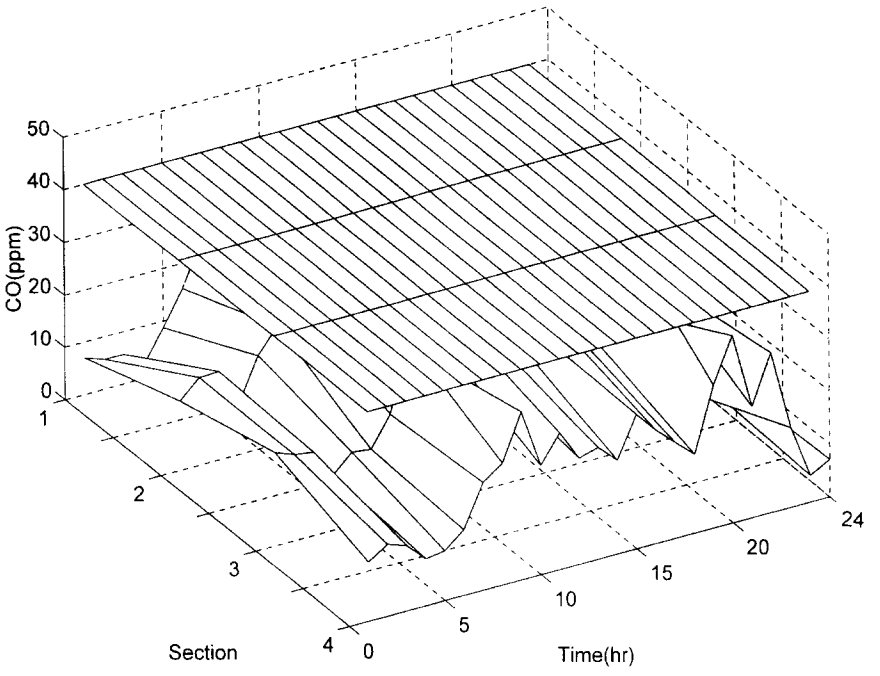

Fig. 25. CO vs. time and tunnel sections (Case 5).

Table 5
PI values for 5 cases

	k_1	k_2	k_3	$\int\int \Delta CO^2\,dx\,dt$	$\int\int \Delta VI^2\,dx\,dt$	$\int\int \Delta N^2_{\mathrm{JFON}}\,dx\,dt$	*PI*	
Case 1	$1/10^4$	1/10	$2/10^3$	1.7520×10^5	167.7390	3.960×10^3	0.6724	
Case 2	$1/10^4$	1/10	$2/10^3$	1.7517×10^5	9.0144	8.556×10^3	0.3611	*
Case 3	$1/10^4$	1/10	$2/10^3$	1.7549×10^5	407.7360	2.130×10^3	0.7020	
Case 4	$1/10^4$	1/10	$2/10^3$	1.7532×10^5	410.6	3.206×10^3	0.6831	
Case 5	$1/10^4$	1/10	$2/10^3$	1.7429×10^5	6.8429	1.350×10^3	0.3564	*

heavy-task individually. Case 2 employs general-task FLC rules. Table 3 with added-on modified membership partition while case 5 employs heavy-task FLC rules Table 4 instead.

How to quantify the performance is based on the following concept:

- Control $CO \leqslant 50$ ppm, the closer to 50 ppm, the better for saving power consumption.
- Control $VI \geqslant 50\%$, the closer to 50%, the better for saving power consumption.

The reason for the above ideas is that there is no need to consume lots of electrical power to make *CO* much less than 50 ppm and VI much higher than 50%.

Fig. 26 shows a profile of power consumption due to operation of jet fans in each station at various time. For a fixed station at fixed time, the power consumption of jet fans depends on their motor starting current and motor running current. Jet fans to be turn on and turn off quite often will resulting in tremendous power loss. Therefore, the number increment of working jet fans to be switched on ΔN_{JFON} should be included in the following quadratic performance index:

$$PI = \int_0^T \int_0^X [k_1 \Delta CO^2(x,t) + k_2 \Delta VI^2(x,t) + k_3 \Delta N^2_{\mathrm{JFON}}(x,t)]\,dx\,dt \tag{52}$$

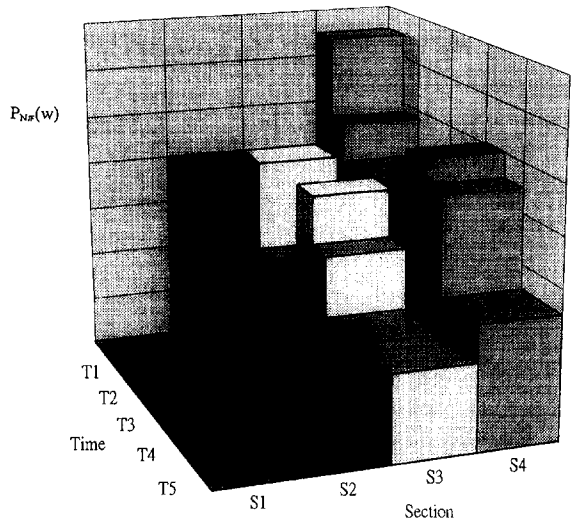

Fig. 26. The power dissipation of jet fans.

where

$T = 24\,(\mathrm{h})$,

$X = 13\,200\,(\mathrm{m})$ (compiled with Fig. 5).

Considering the global performance in Eq. (52), the term ΔCO^2 is integrated with respect to the entire tunnel length and 24 h, so as to the other terms ΔVI^2 and $\Delta N^2_{\mathrm{JFON}}$. Assigning the terms $\int\int \Delta CO^2\,\mathrm{d}x\,\mathrm{d}t$, $\int\int \Delta VI^2\,\mathrm{d}x\,\mathrm{d}t$ and $\int\int \Delta N^2_{\mathrm{JFON}}\,\mathrm{d}x\,\mathrm{d}t$ have equal contribution to the performance index, case 1 is regarded as a reference to select the weighting factors k_1, k_2, and k_3 in terms of normalization. After k_1, k_2, and k_3 are found and fixed, the rest cases, i.e. cases 2–5 are dealt with their performance index, respectively. These five cases then have the same basis to make comparison with each other. In physical meaning, effect of changing k_1, k_2, and k_3 is the same as if changing the membership partition (i.e. changing the control gain).

Table 5 shows the performance index for the above five cases. It is obvious that cases 2 and 5 have less *PI* value; in other words, much better performance.

8. Conclusion

The ventilation problems of a road tunnel are clearly addressed in the introduction. The configuration layout including facility installation, pollutant distribution, sensing elements and control elements is described in detail and compiled with its following positioning of sensing elements and control elements. After the functional environment is set up, fuzzy logic control (FLC) with defined membership functions, inference and defuzzification is then applied to the ventilation control. With the filtering process to deal with space and time, each sectional pollution can be found from a large scope point of view. A thorough environment of ventilation control system is thus established.

As to the computer simulation, five cases categorized into the general-task group and the heavy-task group are taken into account. Simulation results together with performance evaluation point out that the general-task FLC rules are applicable to the general cases with normal forward wind speed and rush-hour traffic while the heavy-task FLC rules are qualified for the heavy-task job with reverse wind speed and traffic congestion. This is the so-called two-level control scheme developed from the computer simulation. The entire tunnel ventilation control system and evaluation is thus fully constructed and proved to be functionally workable.

References

[1] T. Iokibe, N. Mochizuki, T. Kimura, Traffic prediction method by fuzzy logic, Proc. 2nd IEEE Internat. Conf. on Fuzzy Systems, 1993, pp. 673–678.

[2] J. De Rooij, Tunnel monitoring and control system, IEE Coll. on 'Electrical and Electronic Systems for Road Tunnels', 1992, pp. 2/1–7.

[3] K. Nagataki, C. Kotsuji, M. Yahiro, M. Funabashi, H. Inoue, A scheme and operation results of road tunnel ventilation control using hybrid expert system technology, Hitachi Rev. 41 (1) (1992) 51–58.

[4] K. Tamura, N. Matsushita, Experiments on tunnel ventilation controls, Meiden Rev. (International Edition) (2) (1991) 45–50.

[5] M. Funabashi, I. Aoki, M. Yahiro, H. Inoue, A fuzzy model based control scheme and its application to a road tunnel ventilation system, Proc. IECON '91 Internat. Conf. on Industrial Electrics, Control and Instrumentation, vol. 2, 1991, pp. 1596–1601.

[6] T. Koyama, T. Watanabe, M. Shinohara, M. Miyoshi, H. Ezure, Road tunnel ventilation control based on nonlinear programming and fuzzy control, Trans. Inst. Electrical Eng. Japan, 113-D (2) (1993) 160–168.